

Radiofrequency Interference Filters Design Based on Complementary Split Rings Resonators

D. Pérez, I. Gil, and R. Fernández-García

Department of Electronic Engineering, Universitat Politècnica de Catalunya
Colom 1, Terrassa 08222, Spain

Abstract— Low frequency analog and digital electronic circuits are susceptible to radiofrequency interference (RFI). This disturbance is produced when the coupled RF signal is rectified by the non-linear behavior of the semiconductors used in the small signal analog input stages of the electronic system. These circuits present an AM demodulation effect produced by nonlinearity of internal transistors, generating parasitic signals in the low-frequency range and undesired offset voltage. In this paper, an alternative to the current standard EMI filters is presented by combining the conventional printed circuit board layout with complementary split ring resonators (CSRRs), in order to reduce the output offset impact due to RFI. An operational amplifier circuit has been designed with a 4-stage CSRR filter, electromagnetically simulated and experimentally tested. Two prototypes have been implemented, with and without CSRRs in order to compare the filter properties in standard FR4 substrate. The resonance frequency of the CSRRs has been designed in the vicinity of 2.4 GHz in order to prevent susceptibility in the ISM band. Electromagnetic and electrical equivalent circuit model simulations are also provided and compared with experimental results. Measurement data show an effective rejection of the undesired RF demodulation without affecting the signal integrity out of the filter band, and therefore a significant reduction concerning output offset voltage impact in terms of RFI amplitude with no-extra cost in terms of the device area or manufacturing process.

1. INTRODUCTION

Electronic systems are usually disturbed by high frequency radiofrequency (RF) electromagnetic interference (EMI), whose amplitudes change randomly in time. This out of frequency band electromagnetic compatibility (EMC) issue is produced when the RF signal is coupled to sensors and cabling of the system, conducting the EMI to signal-conditioning, and causing errors or malfunction due to the rectification by the non-linear behavior of the semiconductors used in the electronic systems [1].

To solve this problem, effective filtering techniques must be implemented at the input stages of the system in order to avoid the non-desired rectification effect. Standard solutions are based on design robustness (involving a higher number of electronic components) or layout shielding (involving extra metal layers or area) [2]. Recently, specific multilayer layout techniques based on electromagnetic band gaps (EBGs) have appeared in order to filter EMI in several applications with good performance [3]. EBGs belong to a broad family of artificial media with electromagnetic properties generally not found in nature, called metamaterials. A second type of metamaterials, the so-called effective media (i.e., metamaterials satisfying the condition: signal wavelength ($\lambda \ll$ period) have shown some excellent notch filtering properties. Among them, the group called single negative media (SNG) are used in this work in order to implement a filter technique to mitigate RFI.

Physically, SNG (i.e., effective media with negative magnetic permeability $\mu < 0$, or electric permittivity, $\varepsilon < 0$) can be implemented by using so called split-ring resonators (SRRs) and their dual counterparts, the complementary split-ring resonators (CSRRs) [4, 5]. In this paper, a filter developed by means of effective media metamaterials based on CSRRs is used to reduce RFI in a conventional analog circuit constituted of a differential amplifier based on an OPAMP.

2. CSRRs

Essentially, CSRRs (Fig. 1(a)) are the negative images of SRRs. SRRs consist of a pair of metal rings etched on a dielectric slab with apertures in opposite sides which can be mainly excited by means of a parallel magnetic-field along its axis. If an array of SRRs is located close to a transmission line, some current loops can be induced in the rings and they reflect the incident host signal at resonance. Therefore they behave as an LC tank magnetically coupled to the host line [6]. From duality arguments based on an approximation of the Babinet's principle for dielectric boards, it is demonstrated that the CSRRs, roughly behave as their dual counterparts (i.e., their resonance

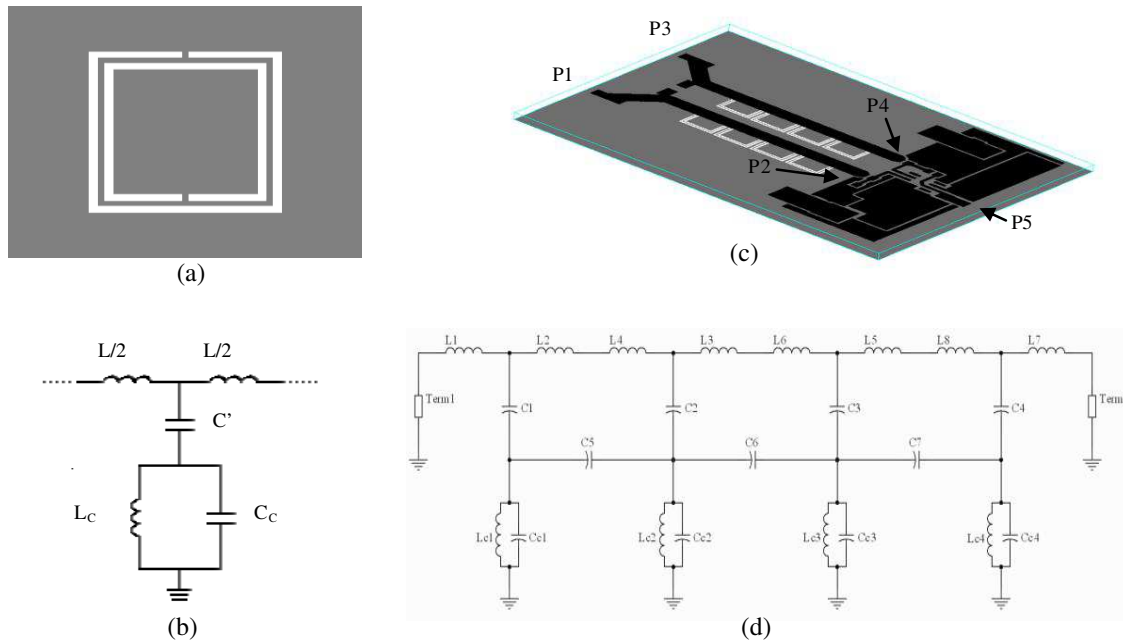


Figure 1: (a) Topology of the CSRR. Metallization zones are depicted in grey. (b) Lumped-element equivalent circuit of the CSRR coupled to a transmission line. (c) Designed layout. The black layer corresponds to the top layer, whereas the grey layer corresponds to ground, where the CSRRs have been etched. (d) Equivalent circuit model of the implemented filter.

frequency is approximately equal to that of the corresponding equivalent SRRs). An efficient way to achieve stop-band frequency responses is to etch CSRRs in the ground plane of a structure such as a microstrip line (or similar) or even in the conductor strip. CSRRs are coupled electrically to the host line according to the model shown in Fig. 1(b). The main advantage of these sub-wavelength particles are their low implementation cost (no extra components, neither PCB layers are required or special etching techniques) and the quasi-non-area consumption, since they are located in the ground plane of the overall structure. With regard to the filtering effectiveness a trade-off between the rejection level and the number of CSRR stages appears.

3. PROPOSED STRUCTURE

The test circuit consists of a conventional differential amplifier. The configuration corresponds to a basic instrumentation amplifier with an output voltage approximately equal to the input voltage difference. In order to avoid RFI reaching the OPAMP input, a 4-CSRR filter has been designed and combined in the final prototype. Fig. 1(c) shows the PCB designed layout. It can be observed two CSRR arrays located in the ground plane, underneath the input transmission lines carrying the signal of interest to the differential input. Notice that this distribution implies effective non-area consumption with respect to a conventional 1-layer design. Moreover, no extra lumped circuitry is needed and no series stage filter is required.

The resonance frequency of the CSRRs has been designed in the vicinity of 2.4 GHz, by means of the *Agilent ADS* and *Momentum* software in order to prevent susceptibility in the Industry-Scientific-Medical (ISM) radio band. In fact, the involved single resonator dimensions have been slightly detuned in order to achieve a wider stop-band bandwidth (i.e., single CSRRs with close resonance frequencies). Therefore, a final simulation step based on a multiple tuning procedure has been developed. EMI filter simulations have been performed between external input ports (P1 and P3) and internal ports (P2 and P4) before OPAMP and circuitry stage (output port corresponds to P5) (Fig. 1(c)).

Figure 1(d) depicts the corresponding full lumped circuit model by taking into account the electrical model illustrated in Fig. 1(b). The inter-resonator coupling between adjacent CSRRs has been modelled by means of capacitances $C5, C6, C7$.

By analyzing a single CSRR coupled to the line (i.e., no inter-resonator coupling), two resonance frequencies arise: the frequency that nulls the shunt impedance (i.e., transmission zero frequency),

given by (1) and the resonance frequency of the CSRR given by (2):

$$f_z = \frac{1}{2\pi\sqrt{L_C \cdot [C_C + C']}}. \quad (1)$$

$$f_0 = \frac{1}{2\pi\sqrt{L_C C_C}}. \quad (2)$$

On the other hand, the periodic structure under study by neglecting inter-resonator coupling, satisfies (3),

$$\cos \varphi = 1 + \frac{Z_S(j\omega)}{Z_P(j\omega)}. \quad (3)$$

This equation allows the analysis of periodic circuits based on the cell depicted in Fig. 1(b) with the help of the dispersion relation and Bloch impedance. φ denotes the phase shift of the elemental cell, and Z_P and Z_S correspond to the shunt and series impedance, respectively, of the T-circuit model. By combining electromagnetic simulation results and Equations (1)–(3) the parameters of the overall model can be extracted.

4. FABRICATED PROTOTYPES

Two experimental prototypes have been fabricated and tested. Both implementations present the same top level metal layer layout and are differentiated from the ground plane (a conventional one in the first case and a ground plane disturbed by etched CSRR arrays in the second case). Fig. 2 shows the prototype setup consisting of a 3-port 4-stage CSRR loaded parallel transmission lines, which have been designed to obtain a stop band filter around 2.4 GHz. The OPAMP used in the prototypes is a UA741CD, supplied by two voltage regulators, a MC78M15BDTG (15 V) and aMC79M15CDTG (−15 V). All resistor values are 1 k Ω . Decoupling capacitors (100 nF and 10 μ F) have been also used to complement the supply lines. The substrate corresponds to the commercial MC 100 FR4. Specifically, 50 Ω two microstrip access lines are considered with dimensions: width $W = 2.84$ mm, length $l = 4$ cm, and separation $s = 6.55$ mm. The total circuit area is 6.9×4.8 cm².

5. EXPERIMENTAL AND SIMULATION RESULTS

In order to test the overall performance of the proposed CSRR prototype, a RFI coupling has been emulated by means of a signal modulated in AM (with carrier frequency $f_C = 2.4$ GHz) with a low frequency tone (modulated frequency $f_m = 10$ kHz). The direct power injection carrier amplitude, corresponds to −10 dBm and the modulation index to 50%. The experimental output spectrum at the low operation frequency (10 kHz) reveals a disturbance on the order of 20 dB for the conventional case (Fig. 3(a)), which is produced by the non-linear behavior of OPAMP. However, the CSRRs prototype completely removes this EMI effect, since the impact of resonators notably filters the undesired noise signal at this frequency. In order to evaluate the effectiveness of the proposed implementation, the DC offset voltage in terms of interference amplitude has also been tested and shown in Fig. 3(b). When the noise signal is injected, a significant increase of the offset with EMI amplitudes higher than −5 dBm is observed in the conventional circuit, whereas in the same conditions, the offset of the prototype equipped with the CSRR filter remains constant (−1.19 mV). Notice also that the offset level is almost 4 times lower in CSRR filtered prototype, since the best offset level for the conventional device is approximately −4 mV.

With regard to the filter performance, Fig. 4(a) shows the detailed fitting between the proposed equivalent circuit frequency response, the electromagnetic simulation and the equivalent circuit

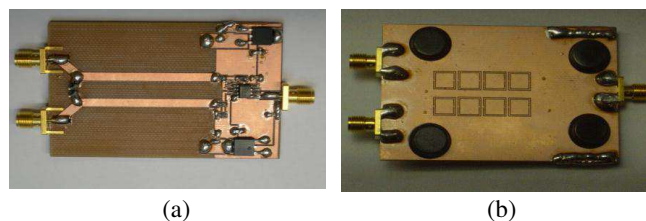


Figure 2: Fabricated prototype device. (a) Top side. (b) Bottom side including CSRRs.

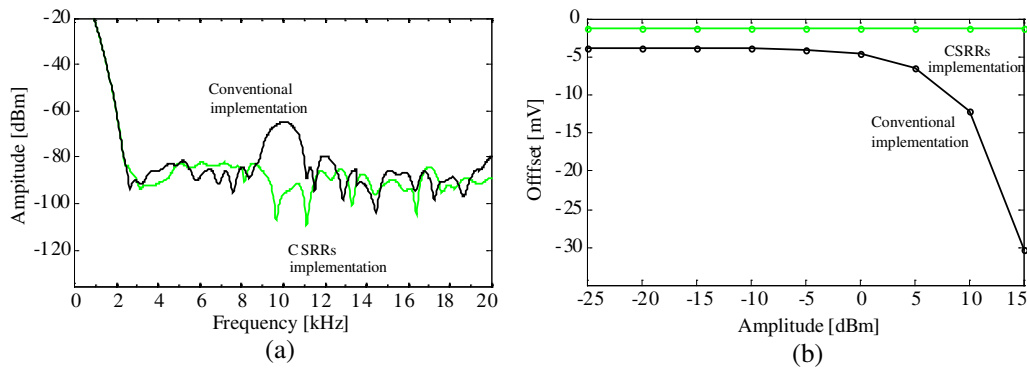


Figure 3: (a) Measured demodulation output device spectrum for conventional and CSRRs prototypes. (b) Measured DC offset vs. RF interference amplitude for conventional and CSRRs prototypes ($m = 50\%$).

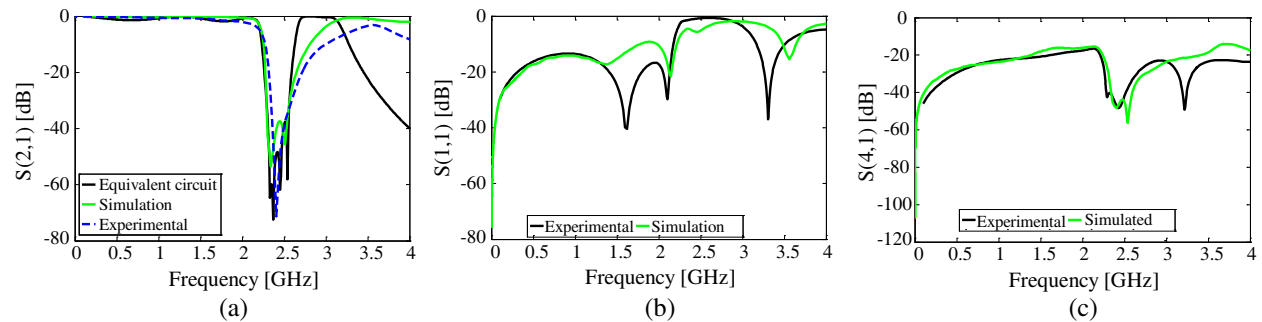


Figure 4: (a) Insertion losses $|S_{21}|$. (b) Return losses $|S_{11}|$. (c) Coupling losses $|S_{41}|$.

model behaviour. As can be observed, a significant rejection level is obtained ($|S_{21}| < -40$ dB) at the frequency band of interest. Fig. 4(b) depicts the CSRRs filter electromagnetic return losses (S_{11}), whereas the crosstalk has been obtained by measuring S_{41} . According to the results, the crosstalk is reduced in the rejection band of the CSRR RFI filter adding an extra benefit in terms of the immunity (coupling reduction).

Moreover, the obtained signal integrity (SI) of the device has been analyzed by means of the eye diagram test including eye width (EW) and eye high (EH). An input test signal of 1 V operating at 50 MHz has been used. The eye diagrams corresponding to the prototype without CSRRs simulated and measured are depicted in Figs. 5(a)–(b). In this case, the obtained values are $EW = 10$ ns and $EH = 999$ mV for simulation and $EW = 10$ ns and $EH = 1.04$ V for measurements. Likewise Figs. 5(c)–(d) show the eye diagram for the prototype with CSRRs. The obtained values by simulation (Fig. 5(c)) are $EW = 9.98$ ns and $EH = 999$ mV and $EW = 10$ ns and $EH = 1.032$ V for measurements (Fig. 5(d)). Thus, the experimental degradation between the prototype with CSRRs and a continuous ground plane reference board of the EW is null whereas a 0.77% difference is observed for the EH . Therefore, an extremely low SI degradation (negligible) is achieved with CSRRs by obtaining with a good filtering response. Therefore, those results reveal an excellent behavior in terms of SI.

6. CONCLUSIONS

In summary, it has been demonstrated that EMI effects due to random RF disturbance signals reaching the OPAMP input circuits, which present an inherent non-linear behavior, can be significantly reduced by means of filters based on CSRR with no impact in terms of signal integrity. Basically, the demodulated low frequency signal attenuation as well as DC offset minimization has been tested, both by simulation and experimentally. In fact, ground loaded CSRR transmission lines can be a compact-low-cost method in order to significantly decrease the PCB RF coupling interference at the ISM band. Simulated and experimental results show a 45 dB coupling reduction at 2.4 GHz. Moreover, it has been demonstrated that CSRRs do not affect the signal integrity out of the filter band since no significant impact is measured in the eye diagram concerning the comparison between both fabricated prototypes.

The authors are confident about the application of these structures for EMI reduction in planar

electronic circuits operating at high frequencies/data-transmission rates.

ACKNOWLEDGMENT

This work has been supported by the Spain-MINECO under Project TEC2010-18550 and AGAUR 2009 SGR 1425.

REFERENCES

1. Gago, J., J. Balcells, D. González, M. Lamich, J. Mon, and A. Santolaria, “EMI susceptibility model of signal conditioning circuits based on operational amplifiers,” *IEEE Transactions on Electromagnetic Compatibility*, Vol. 49, 849–859, Nov. 2007.
2. Lovat, G. and S. Celozzi, “Shielding effectiveness of planar negative-permeability screens,” *IEEE International Symposium on Electromagnetic Compatibility*, 1–6, Detroit, USA, Aug. 2008.
3. Iravani, B. M. and O. M. Ramahi, “Design, implementation and testing of miniaturized electromagnetic bandgap structures for broadband switching noise mitigation in high-speed PCBs,” *IEEE Transactions on Advanced Packaging*, Vol. 30, 171–179, May 2007.
4. Gil, I. and R. Fernández, “Comparison between complementary split ring resonators and electromagnetic band-gap as EMI reduction structures,” *Proceedings of the European Symposium on EMC*, 895–898, Wrocław, Poland, Sep. 2010.
5. Liu, K. Y., C. Li, and F. Li, “A new type of microstrip coupler with complementary split-ring resonator (CSRR),” *PIERS Online*, Vol. 3, No. 5, 603–606, 2007.
6. Baena, J. D., J. Bonache, F. Martín, R. Marqués, F. Falcone, T. Lopetegui, M. A. G. Laso, J. García-García, I. Gil, M. Flores Portillo, and M. Sorolla, “Equivalent-circuit models for split-ring resonators and complementary split-ring resonators coupled to planar transmission lines,” *IEEE Transactions on Microwave Theory and Techniques*, Vol. 53, 1451–1461, Apr. 2005.